C3M and surface radiation budget

Seiji Kato[1], Kuan-Man Xu[1], Takmeng Wong[1],
Norman G. Loeb[1], Fred G. Rose[2], David A. Rutan[2],
Kevin E. Trenberth[3], Tyler J. Thorsen[1], Seung-Hee Ham[2],
Sunny-Sun Mack[2], Yan Chen[2], and Walt Miller[2]

[1]NASA Langley Research Center
[2]Science System & Applications Inc.
[3]National Center for Atmospheric Research

CALIPSO-CloudSat Ten-Year Progress Assessment and Path-Forward workshop
June 8-10, 2016
Paris France

Outline of this talk

- Accomplishments on surface radiation budget
- Status of the surface energy balance residual
- Atmospheric column energy balance
- Cloud type associated with large energy balance residual
- Thoughts on future active sensor missions in order to improve surface radiation budget

Low-level cloud fraction comparison (Jan. 2010)

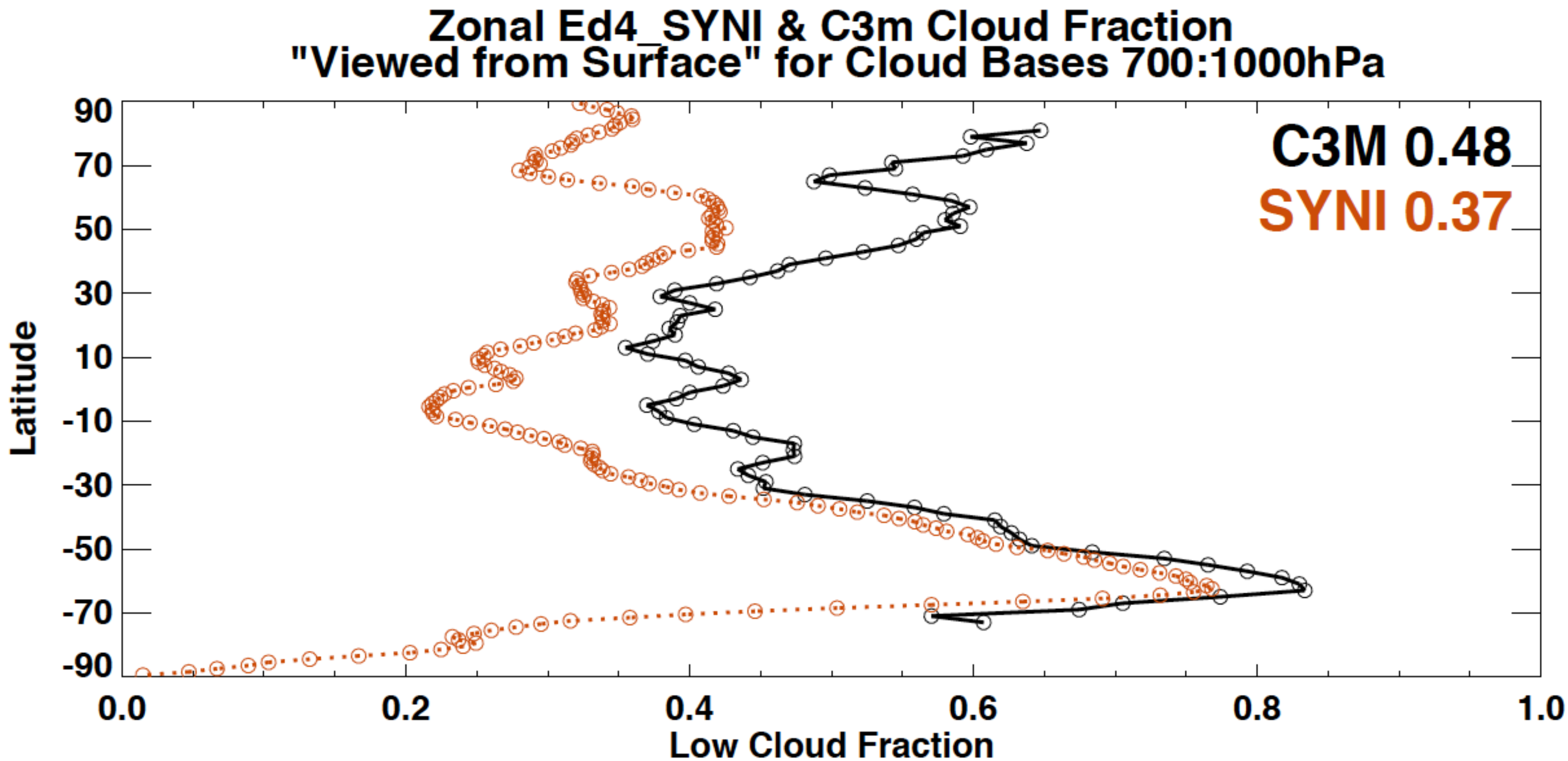

- Low-level cloud fraction derived from passive sensor is under estimated because of cloud overlap
- CALIPSO/CloudSat cloud vertical profiles are used to correct low-level cloud fraction derived from passive sensor for surface irradiance computations

Polar surface radiation budget improvement by CALIPSO and CloudSat

Daytime longwave

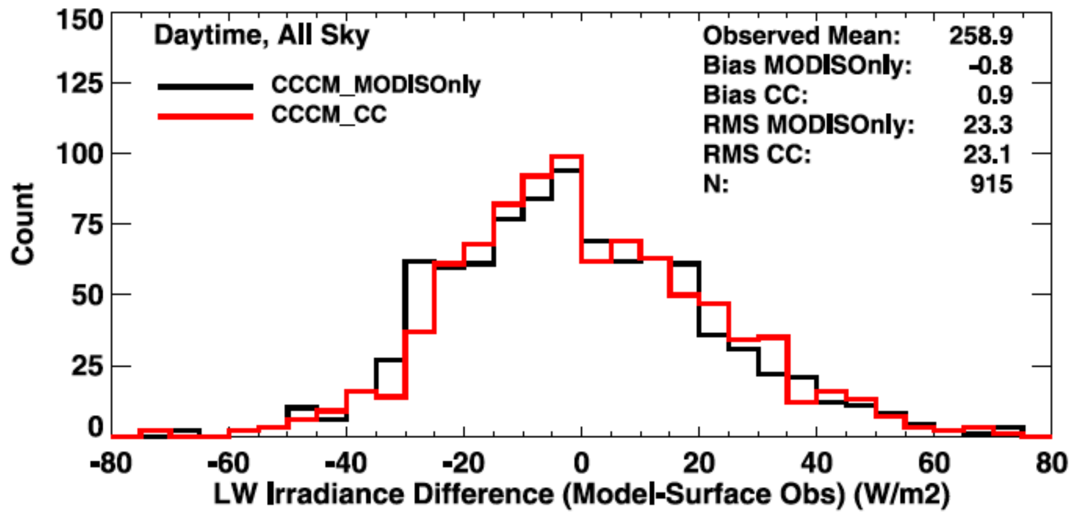

Nighttime longwave

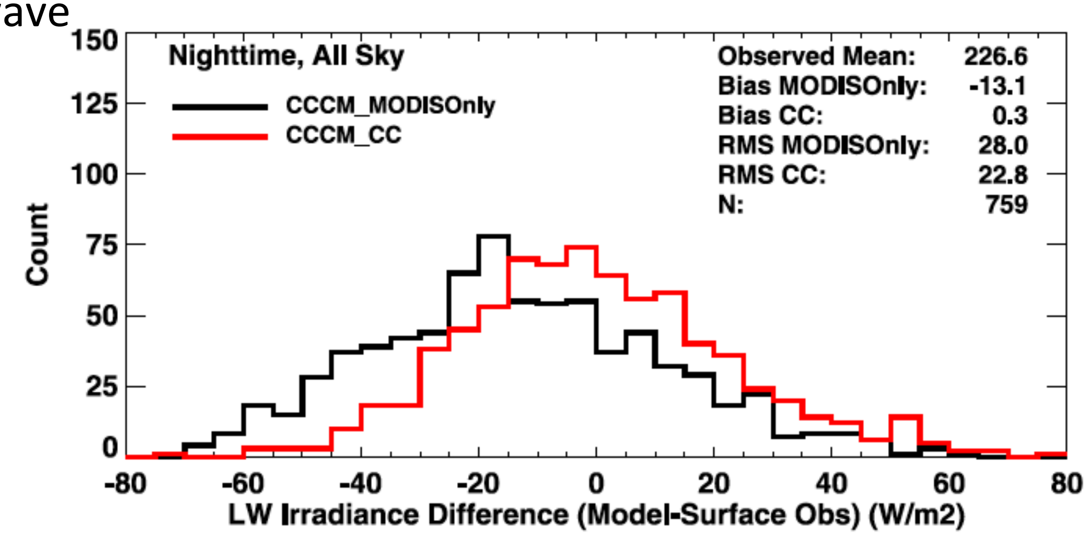

Kato et al. 2011

Global annual mean energy budget

CALIPSO and CloudSat observations reduced the uncertainty in surface radiation budget

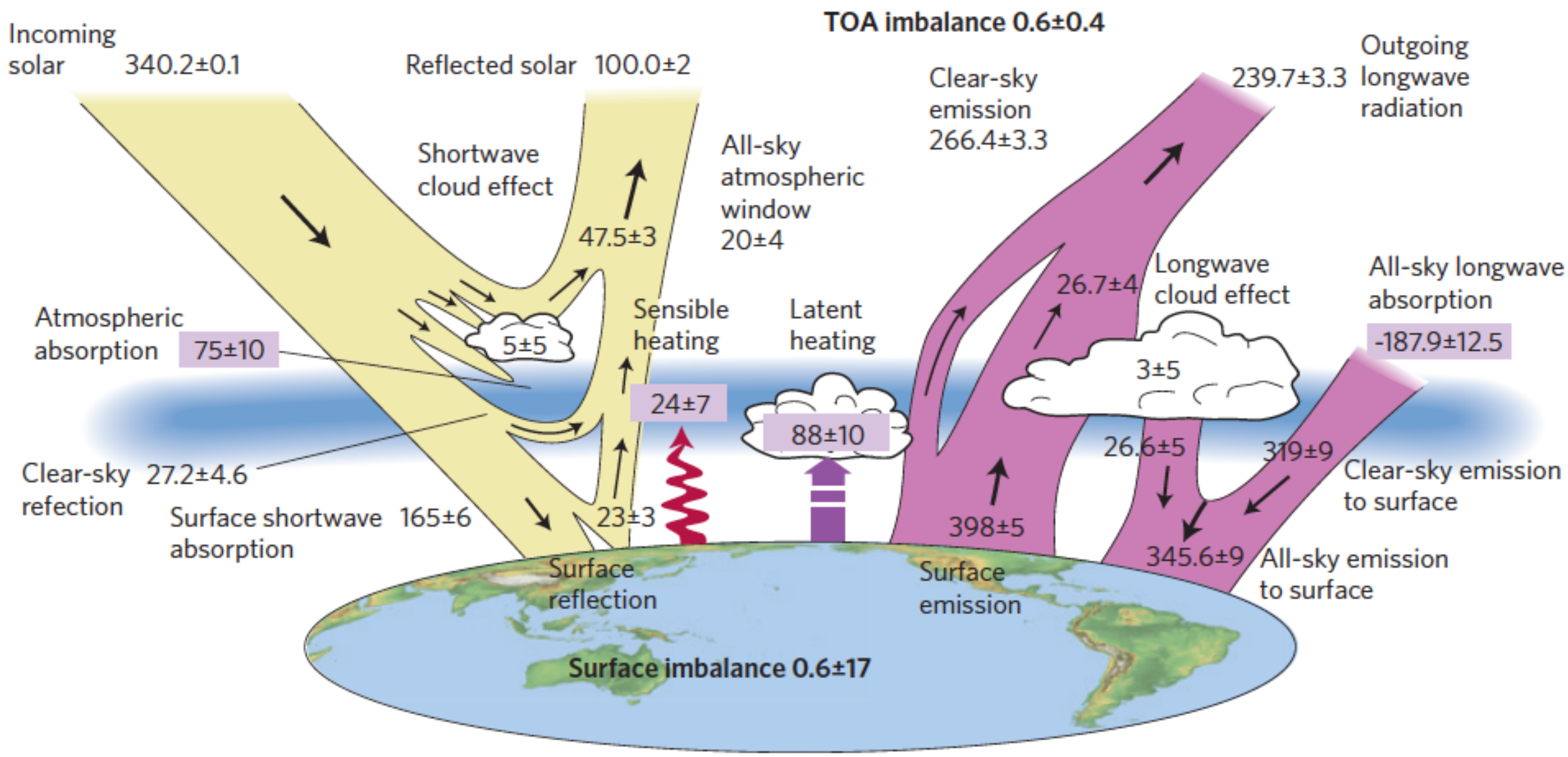

Stephens et al. 2012

Current status of satellite based surface energy imbalance in Wm^{-2}

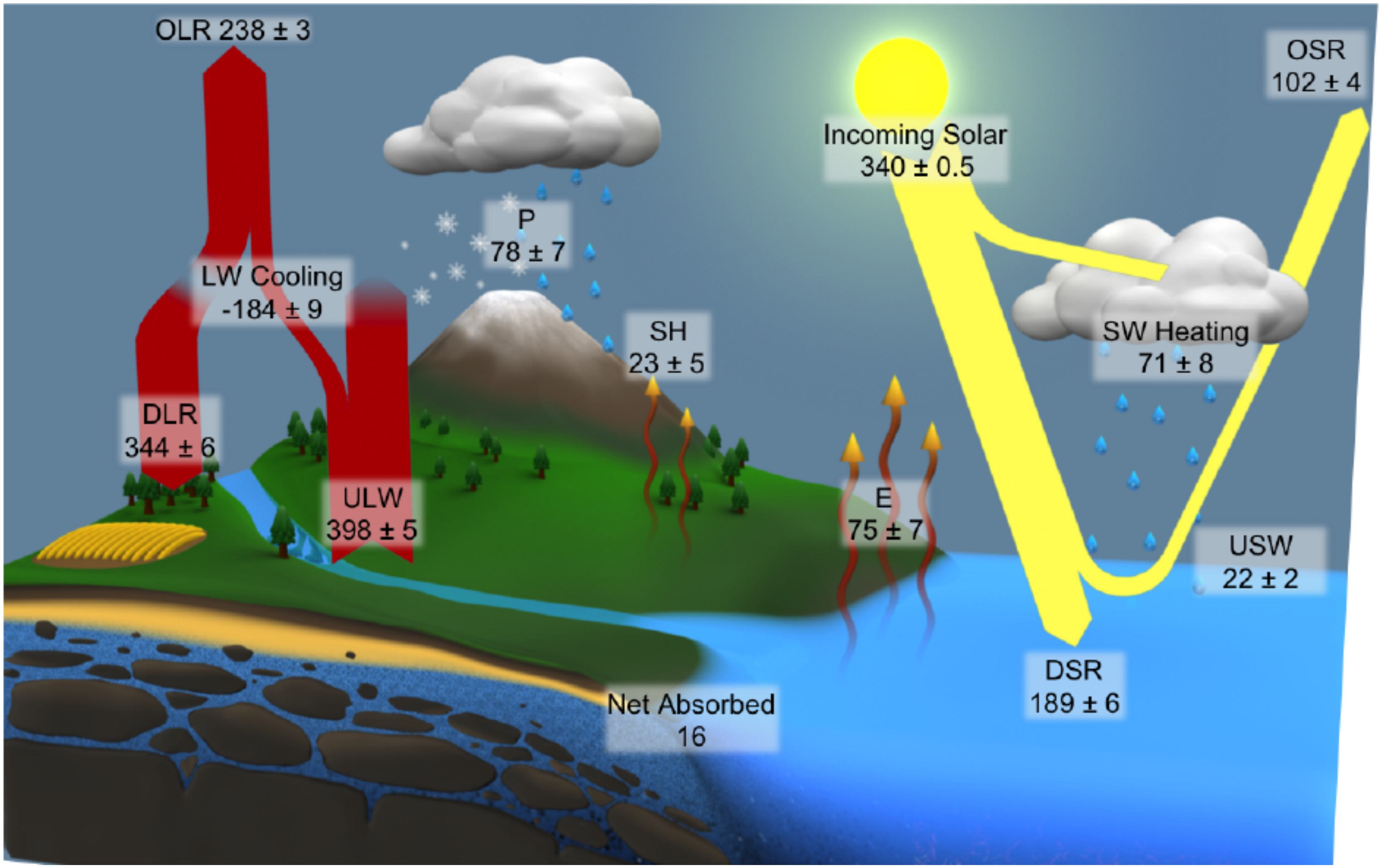

L'Ecuyer et al. 2015 (J. Climate)

Surface: 344-398-23-75+189-22=15 Wm^{-2} (depending on data sets used)
Ocean heating rate: 0.53 to 0.75 Wm^{-2} (Lyman et al. 2010 Nature)

Regions with a large energy imbalance

Atmospheric energy balance (Trenberth and Stepaniak 2003)

$$-\left[\frac{\partial(K_E + S_H + \Phi_s + L_E)}{\partial t} - (R_T - R_s) + H_s + LE + \nabla_p \cdot (\mathbf{F}_K + \mathbf{F}_{DE} + \mathbf{F}_{LE})\right] = 0$$

Water mass balance

$$-\left[\frac{\partial L_E}{\partial t} + LP + LE + \nabla_p \cdot \mathbf{F}_{LE}\right] = 0$$

$$-\frac{\partial(K_E + S_H + \Phi_s)}{\partial t} - \nabla_p \cdot (\mathbf{F}_K + \mathbf{F}_{DE}) + (R_T - R_s) + LP - H_s = 0$$

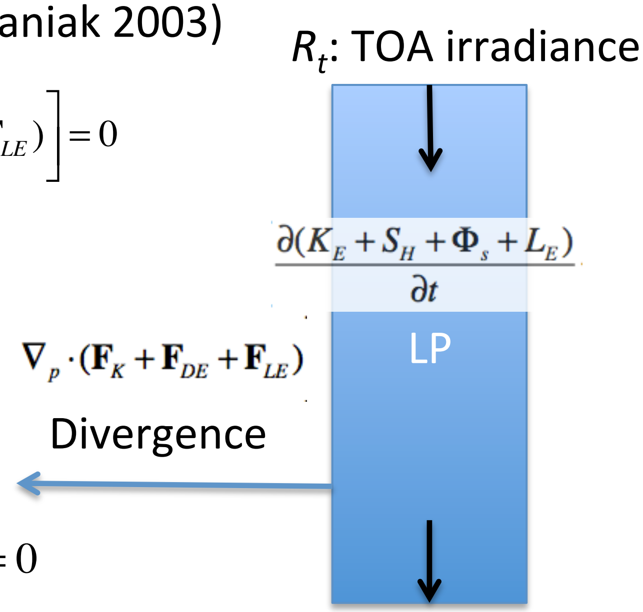

- Kinetic energy + dry static energy tendency
- Kinetic energy divergence
+ atmospheric net irradiance
+ precipitation × (latent heat of vaporization)
- Surface sensible heat flux (positive downward)

R_s: Surface irradiance
H_s: Sensible heat flux
LE: latent heat flux

Neglecting water phase change (the error in the global mean is about 0.8 Wm^{-2})

Testing atmospheric energy balance using observations
Data source (March 2000 through Feb. 2010)

- Atmospheric net irradiance: EBAF-TOA and EBAF-surface (Ed 2.8, Loeb et al. 2009, 2012; Kato et al. 2013)
- Precipitation: GPCP (V2.2, Huffman et al. 1997; Adler et al. 2012)
- Surface sensible and latent heat flux: SeaFlux (Jan 2000 through Dec. 2007, Clayson and Bogdanoff 2014).
- ECMWF ERA-interim Divergence of dry static energy: ERAI.DSEDIV (Trenberth et al. 2011)
- Divergence of kinetic energy: ERAI.KEDIV
- Divergence of latent energy: ERAI.LEDIV
- Total energy tendency: ERAI.TETEN
- Latent energy tendency: ERAI.LETEN

Atmospheric energy components

Net irradiance

Precipitation rate

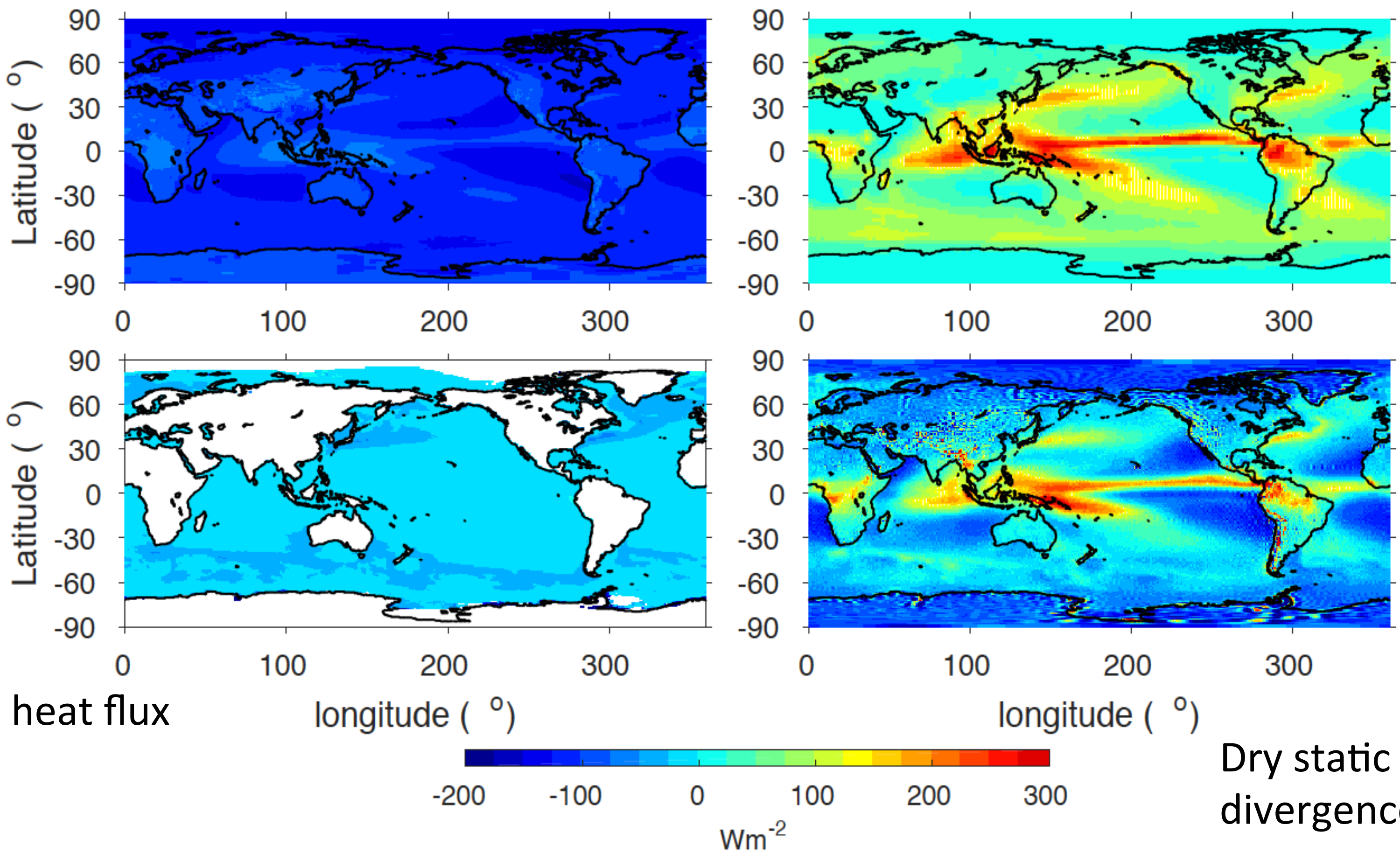

Sensible heat flux

Dry static energy divergence

Sum of all energy terms for the atmospheric column in Wm^{-2} (10 year average)

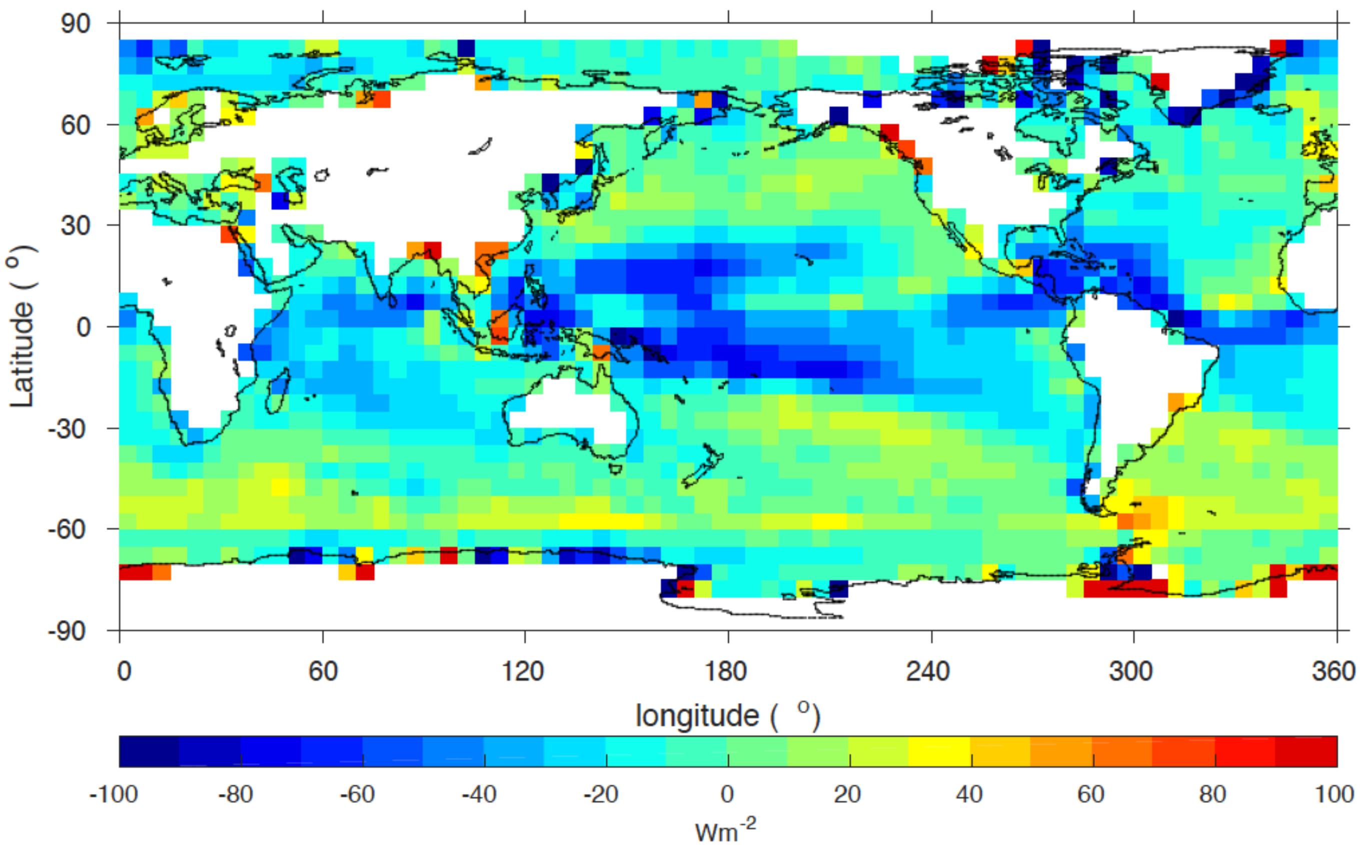

Negative area

- Precipitation is too small
- Divergence is too large
- Radiative cooling is too large
- Upward sensible heat flux is too small

Kato et al. 2016 Submitted to J. Climate

-Dry static and Kinetic energy tendency - divergence of dry static energy -divergence of kinetic energy + atmospheric net irradiance + precipitation - surface sensible heat flux (positive downward)

$$-\frac{\partial(K_E + S_H + \Phi_s)}{\partial t} - \nabla_p \cdot (\mathbf{F}_K + \mathbf{F}_{DE}) + (R_T - R_s) + LP - H_s = 0$$

Cloud object type definitions

Table 2: Cloud object type and selection criteria. Note that cloud objects are derived using only daytime data. Note also that 440 hPa and 680 hPa pressure levels are approximately 7 km and 3.4 km above the sea level in the tropics, respectively.

Cloud object type*	Cloud top height	Cloud optical depth	Cloud fraction	Current Latitude band
Tropical deep convection	< 440 (hPa)	> 10	1.0	25°S-25°N
Trade/shallow cumulus	> 680 hPa	—	0.1 – 0.4	40°N-40°S
Transition stratocumulus	> 680 hPa	—	0.4 – 0.99	40°N-40°S
Solid stratus	>680 hPa	—	0.99 – 1.0	40°N-40°S
Altocumulus	440 hPa < h < 680 hPa	—	0.1 – 0.4	40°N-40°S
Transition altocumulus	440 hPa < h < 680 hPa	—	0.4 – 0.99	40°N-40°S
Solid altocumulus	440 hPa < h < 680 hPa	—	0.99 - 1.0	40°N-40°S
Cirrus	< 440hPa	< 10	0.1 – 0.4	40°N-40°S
Cirrocumulus	< 440 hPa	< 10	0.4 – 0.99	40°N-40°S
Cirrostratus	< 440 hPa	< 10	0.99 – 1.0	40°N-40°S

* All cloud object types of given type are grouped into three size categories, 100 km to 150 km, 150 km to 300 km, and greater than 300 km.

Spatial distribution of Number of cloud objects

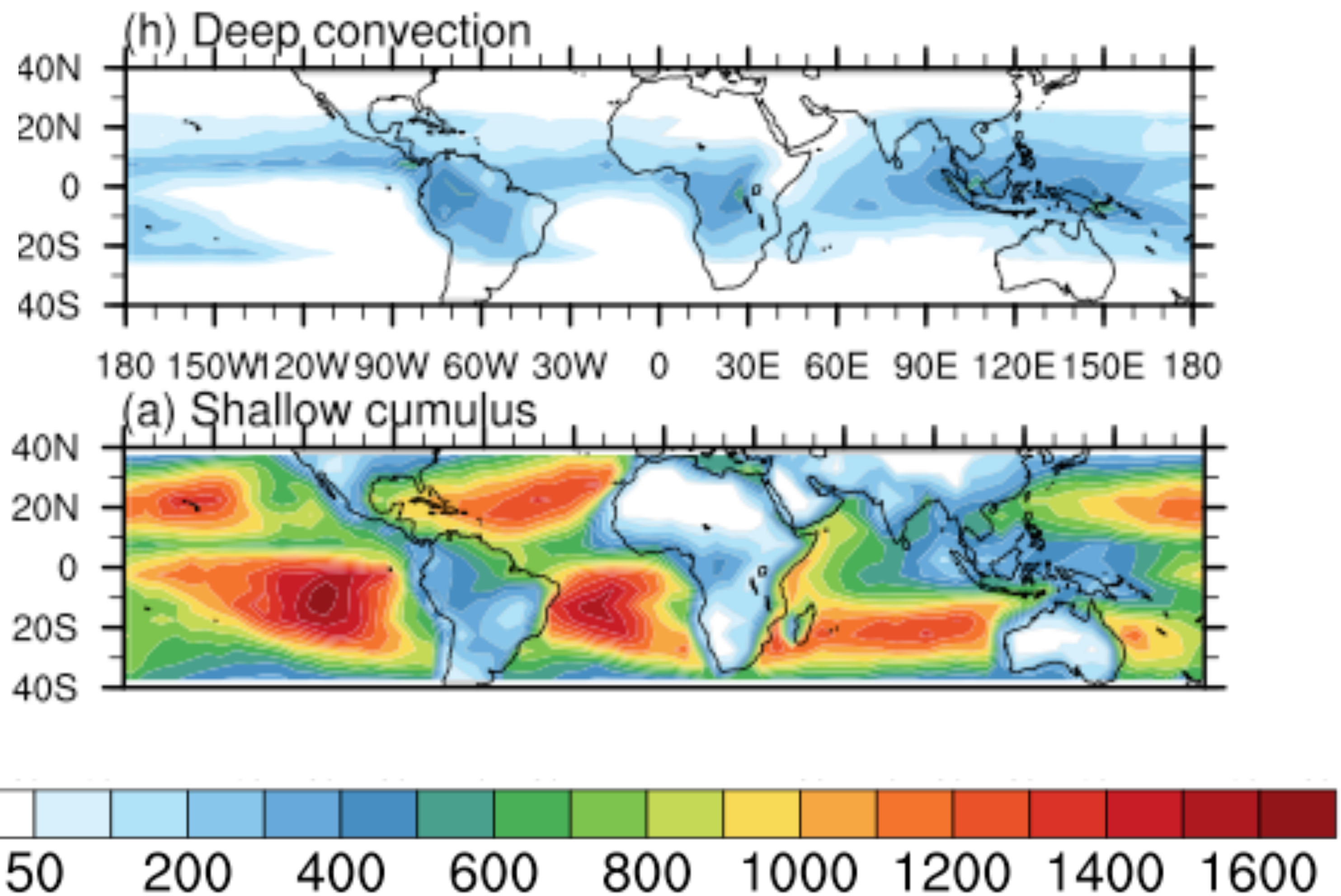

Xu et al. 2015

Seasonal variability of atmospheric energy balance residual vs. deep convective clouds

Southern western Pacific (0° to 25°S; 105°E to 180°E)

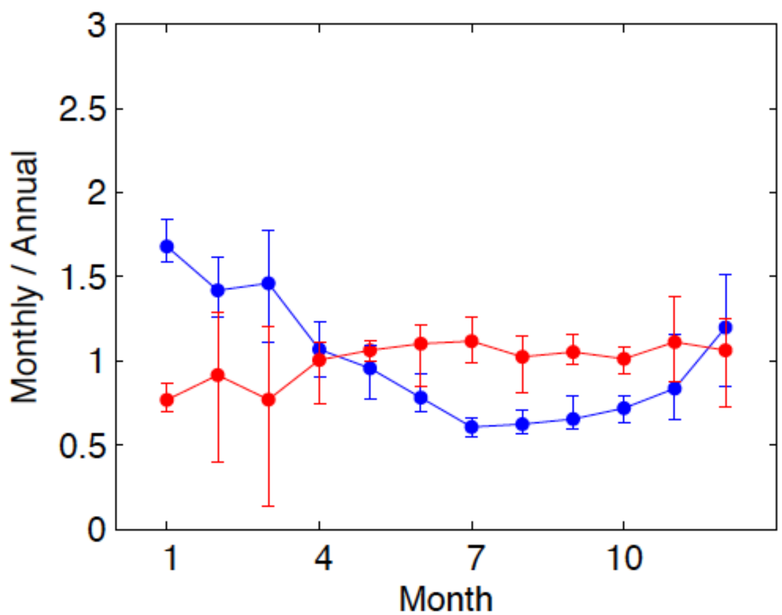

Northern western Pacific (0° to 25°N; 105°E to 180°E)

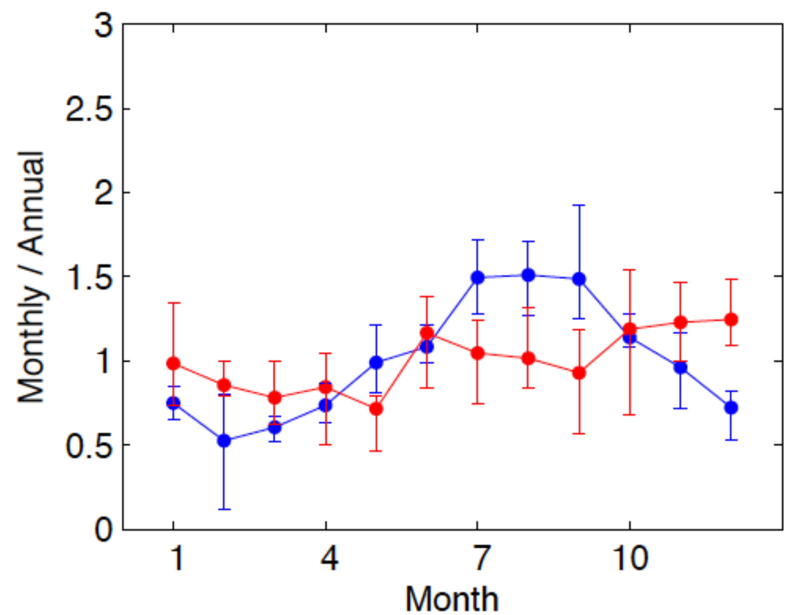

Blue: number of deep convective cloud objects

Red: Atmospheric energy balance residual + surface sensible heat flux

Atmospheric energy balance residual vs. shallow cumulus clouds

NH western Pacific

NH eastern pacific

SH western pacific

SH eastern pacific

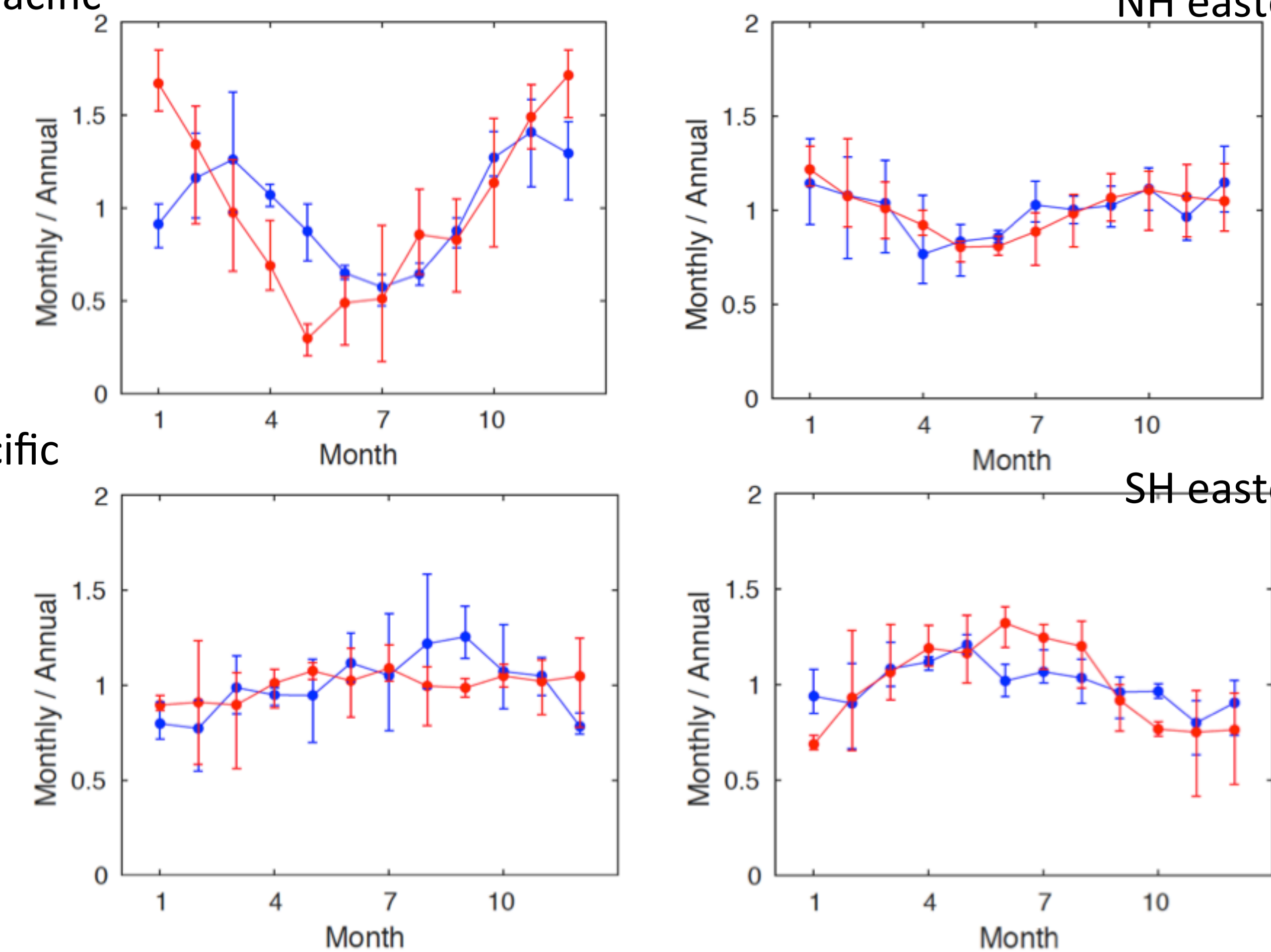

Blue: number of deep convective cloud objects

Red: Atmospheric energy balance residual + surface sensible heat flux

Proposed relationship between shallow cumulus and precipitation by deep convective clouds

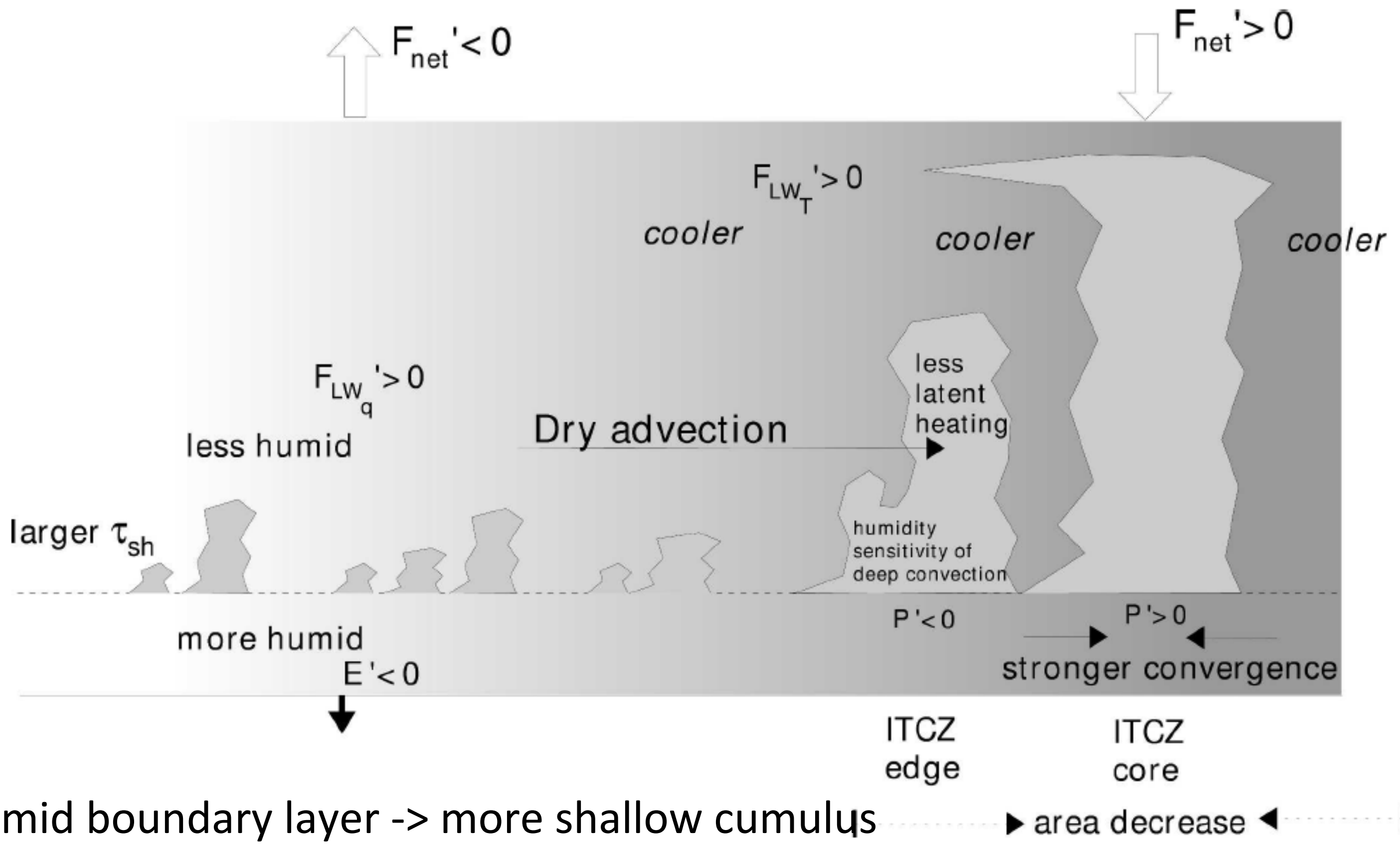

More humid boundary layer -> more shallow cumulus
-> dryer free troposphere -> narrower ITCZ
-> stronger precipitation by deep convective clouds

Neggers et al. 2007 J. Climate

A hypothesis

- A study by Berg et al. (2010) shows that the precipitation rate over tropical eastern Pacific estimated from the CloudSat radar that is not included in the estimate from the TRMM radar is about 0.4 to 0.5 mm day^{-1}, which is ~13 Wm^{-2}, although the 150 km radius range over Barbuda area-averaged precipitation rate by shallow cumuli estimated by Nuijens et al. (2009) reaches about 35 Wm^{-2}.
- Kato (2009) shows that the atmospheric cooling by clouds with the top height pressure greater than 665 hPa is 0 to -25 Wm^{-2} over tropics. According to Oreopoulos et al. (2014) low-level clouds account for roughly 50% of clouds present in cloud regime 2. These lead to about a 10 Wm^{-2} contribution to atmospheric cooling by shallow cumulus clouds.
- Enhanced intense precipitations within deep convective clouds are missed by satellite observations
- It is also possible that cumulus congestus are sometimes present under cirrostratus.

Horizontal distributions of the total number of satellite footprints of deep convective cloud objects in 5° × 5° grids as a function of MJO phases (Phases 1 to 8 from the top to the bottom).

Phase 1

Phase 2

Phase 3

Phase 4

Phase 5

Phase 6

Phase 7

Phase 8

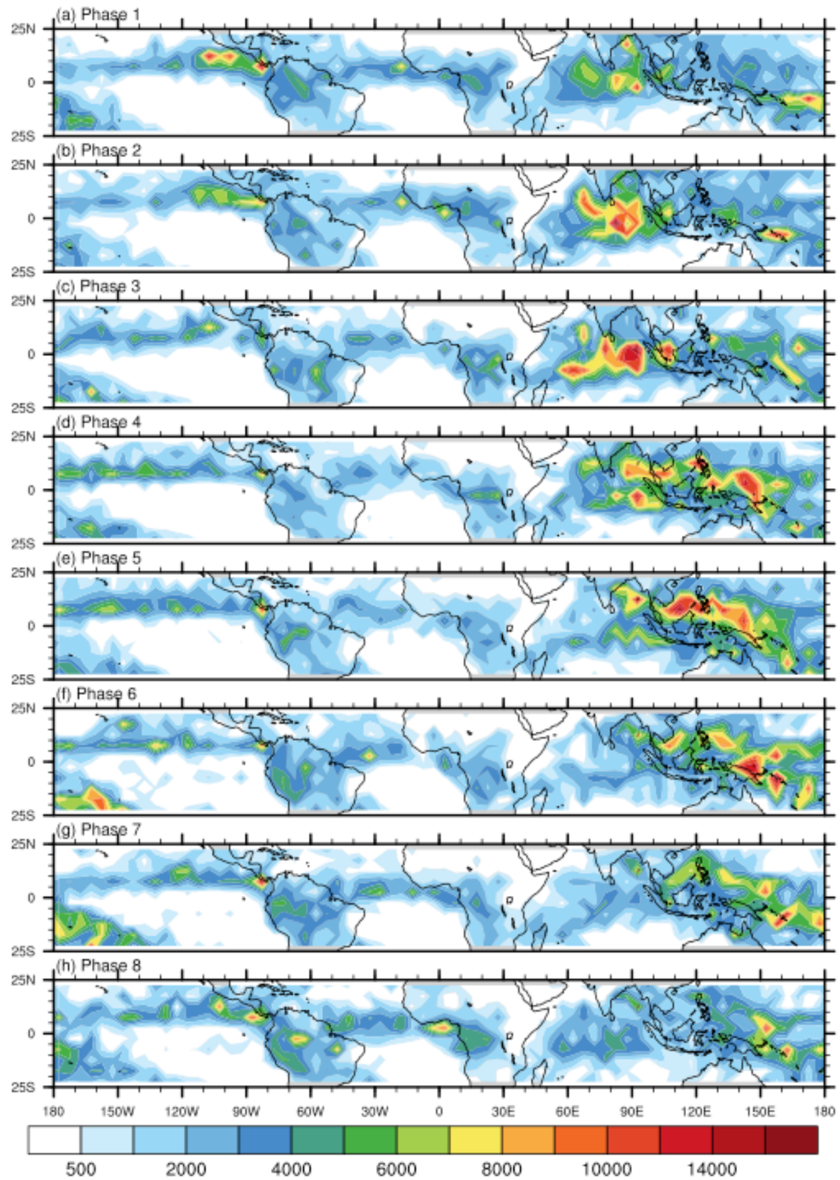

Number of shallow cumulus cloud objects vs. deep convective cloud object size

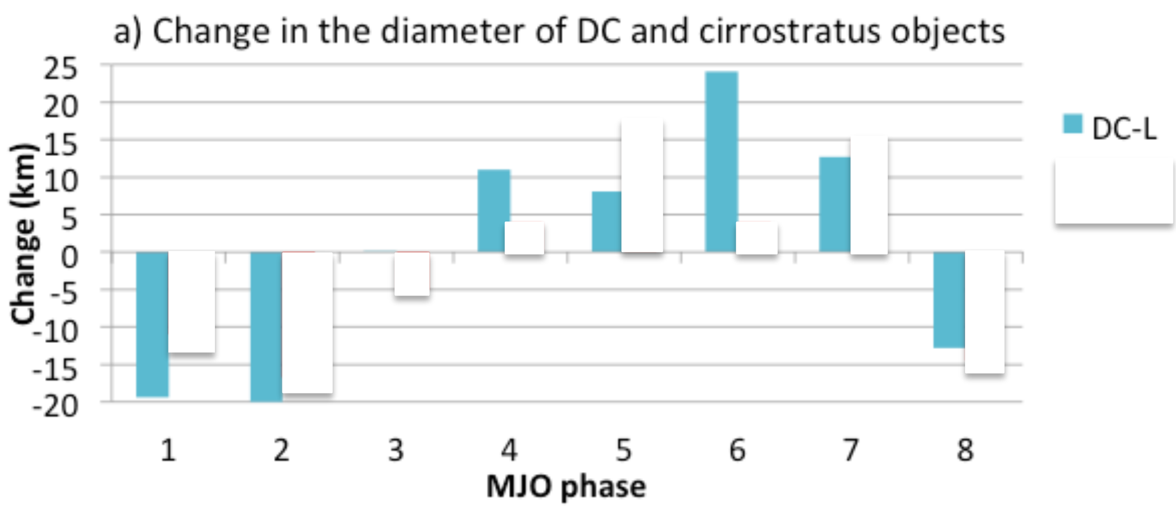

DC-L: large deep convective clouds

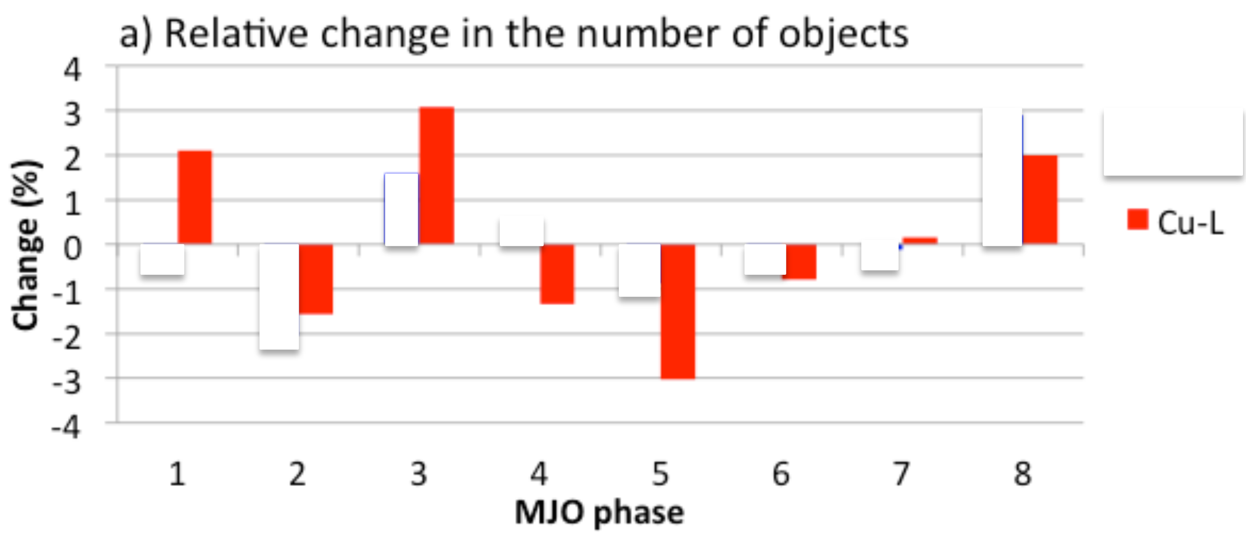

Cu-L: Large shallow cumulus

Xu et al. (2016)

Atmospheric irradiance divergence vs. precipitation anomalies

Radiation is probably not responsible for the 15 Wm^{-2} surface energy balance residual, but the error in anomalies is less certain.
Current accuracy level is ~0.8 Wm^{-2} per decade (at a 60% confidence level) for both surface downward LW and SW irradiances (CERES white paper) while precipitation changes at the rate of ~0.3 Wm^{-2} per decade (2% K^{-1})

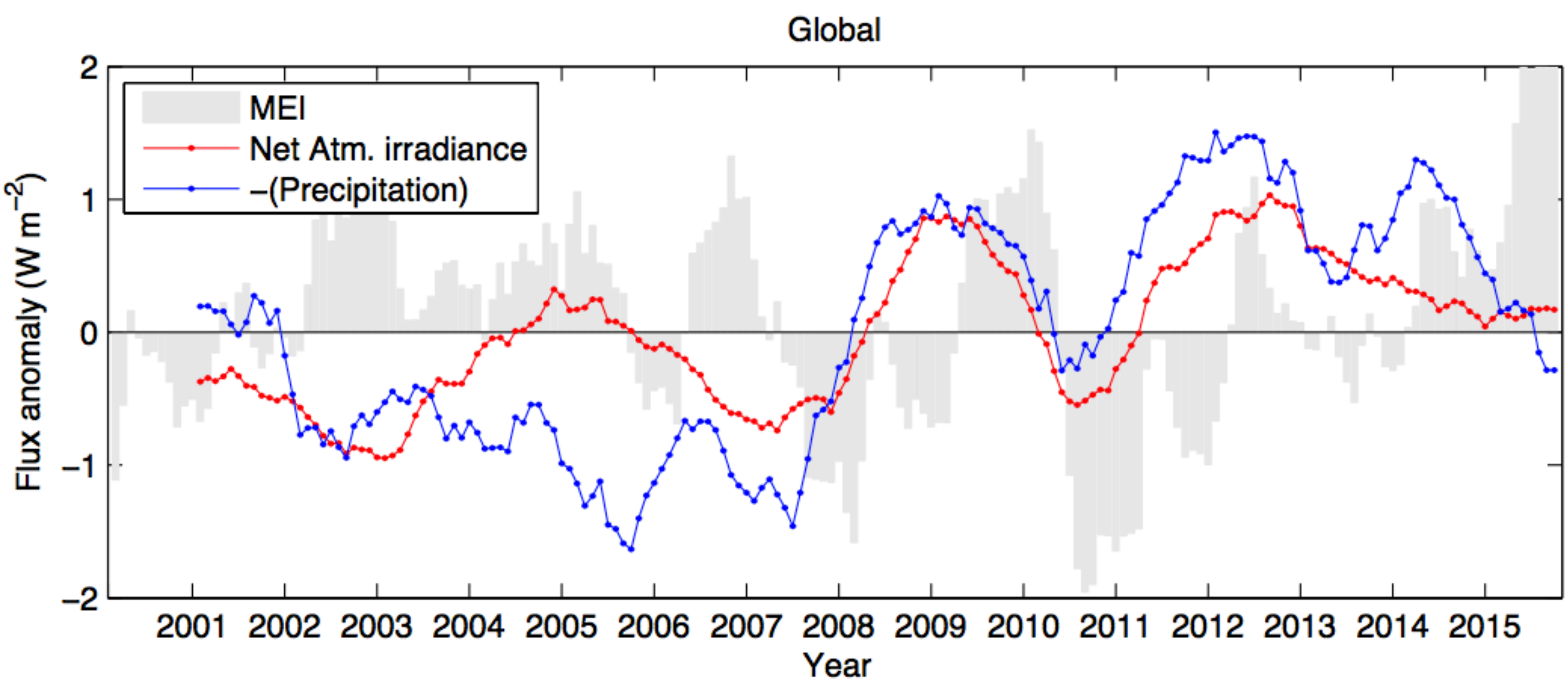

With 12 month running mean
Surface sensible heat anomalies are missing

Future

- Energy in the earth system takes various forms.
- Need to monitor how energy flow through the earth system will be altered under radiative forcing.
- No single instrument can monitor all energy fluxes. We need both passive and active sensors to monitor variability accurate enough (A-train like constellation to preserve co-variability at high temporal resolutions).
- Change in the energy flow is driving climate sensitivity (Otto et al. 2013, Nature Geoscience).

Future improvements of surface radiation budget anomalies active sensors

- Cloud property (fraction, height) constraint to those derived by passive sensors
  - Continuation of observations similar to CALIPSO/CloudSat (especially for polar regions)
  - Enhanced MODIS retrieval (use CALIPSO/CloudSat derived cloud information to initialize MODIS retrieval)
- Use knowledge of better cloud fields to improve temperature and humidity profiles
  - Better boundary temperature and humidity profiles over stratocumulus regions than those provided by reanalyses
  - Better spectral radiative kernels (spectral fingerprinting)

Boundary layer lapse rates derived from CALIPSO and MODIS

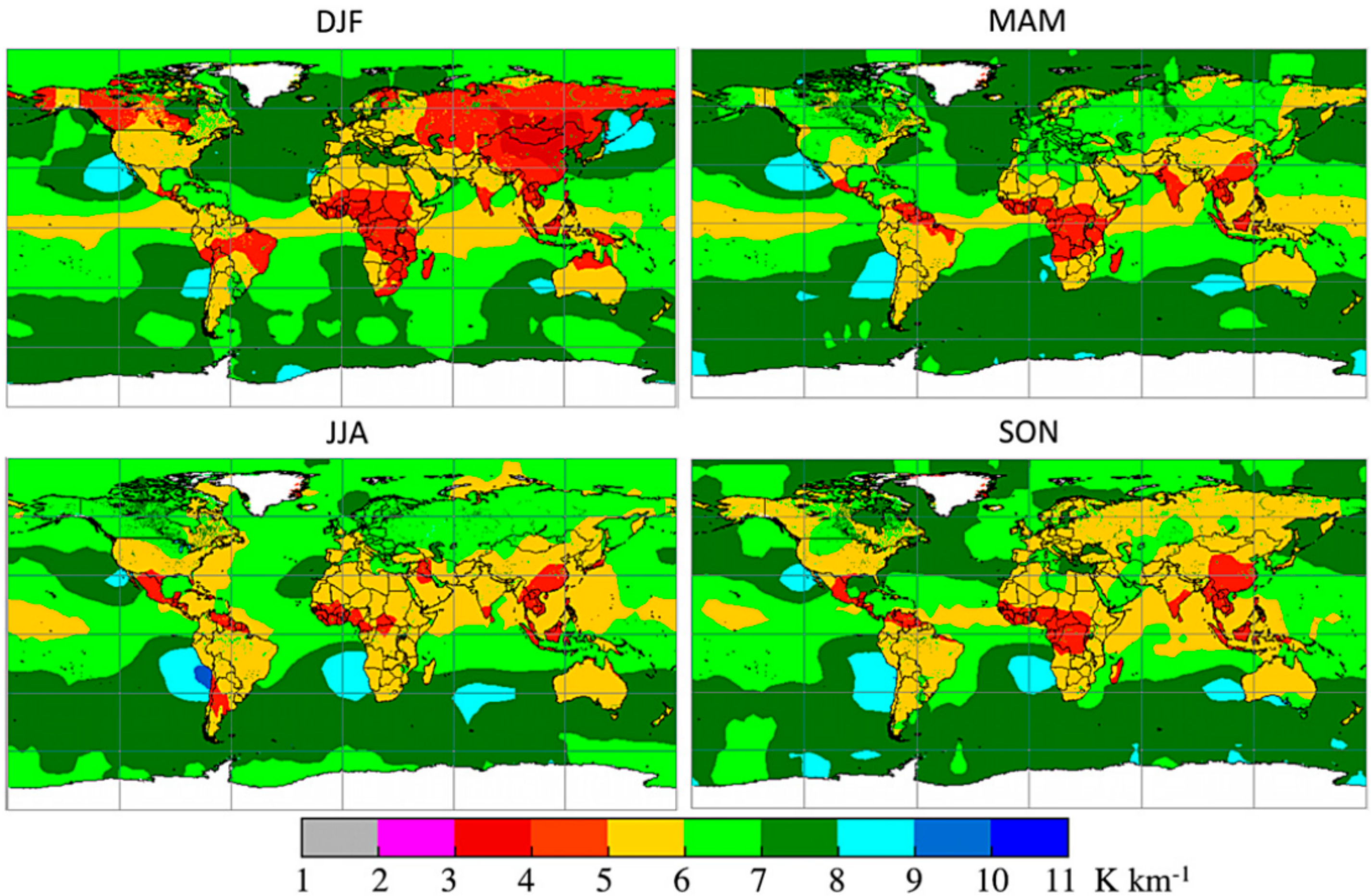

FIG. 6. Daytime boundary layer lapse rates (K km^{-1}) over snow–ice-free scenes for DJF, MAM, JJA, and SON: July 2006–June 2007 and June 2009–May 2010 (2 yr).

Sun-Mack et al. 2014 JAMC

To improve boundary layer cloud top height retrieval from passive sensors

Boundary T and Td corrections

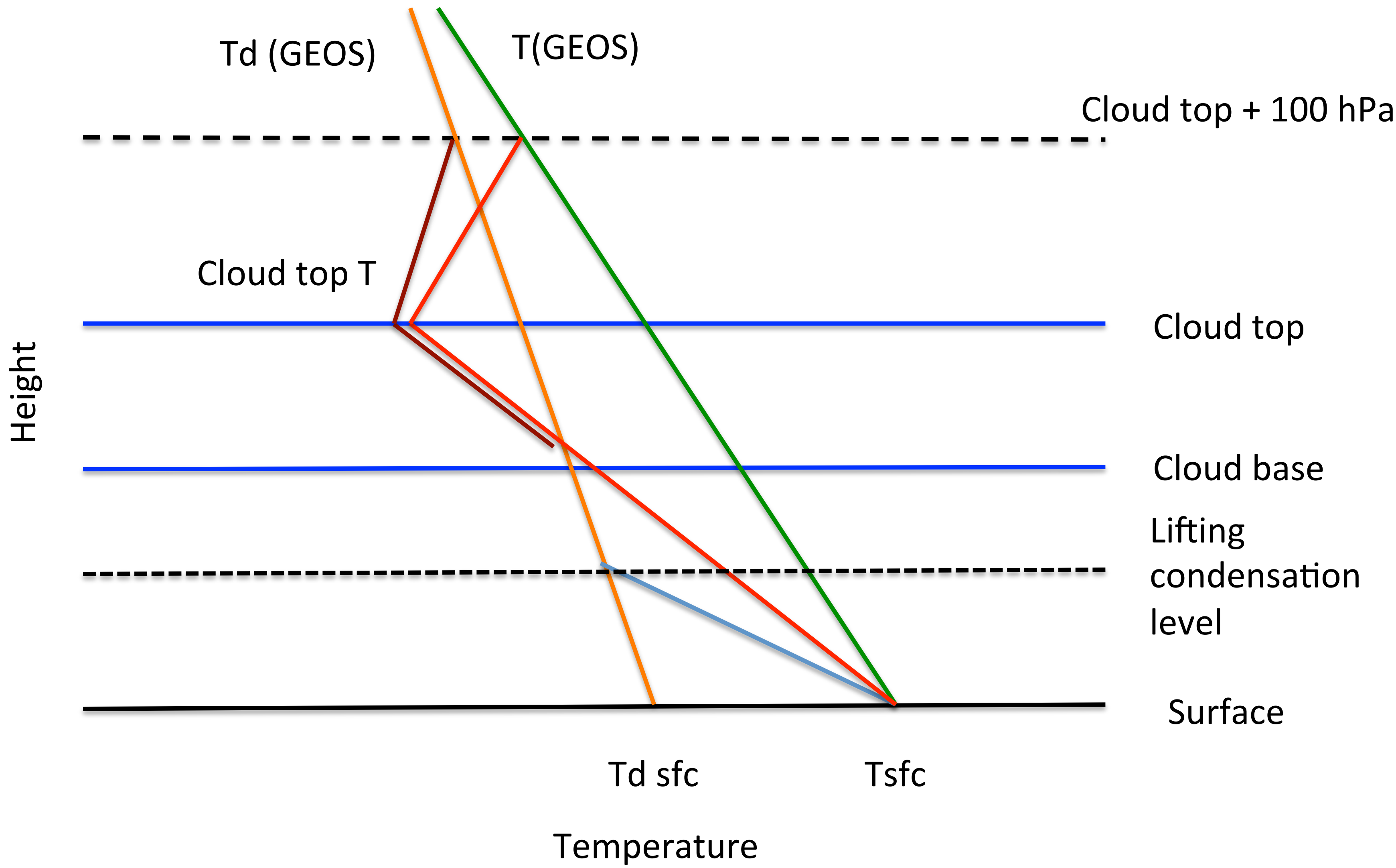

Summary and Conclusions

- Larger regional atmospheric column energy balance residuals exist over tropical ocean
- Atmospheric energy balance residual temporally correlates well with the number of shallow cumulus cloud objects
- A reduction in the mixing time scale of shallow convection leads to more humid mixing layer, dryer free troposphere, a narrower ITCZ, stronger large-scale convergence, and more intense convection (Neggers et al. 2007).
- One possibility is that more intense precipitation within ITCZ is not detected by satellite instruments.
- Monitor energy flow change with passive + active sensors in the future

Back-up slides

Regional energy balance residual (imbalance)

Precip.+Rad.-DSEDIV-KEDIV-TETEN+LETEN+SH

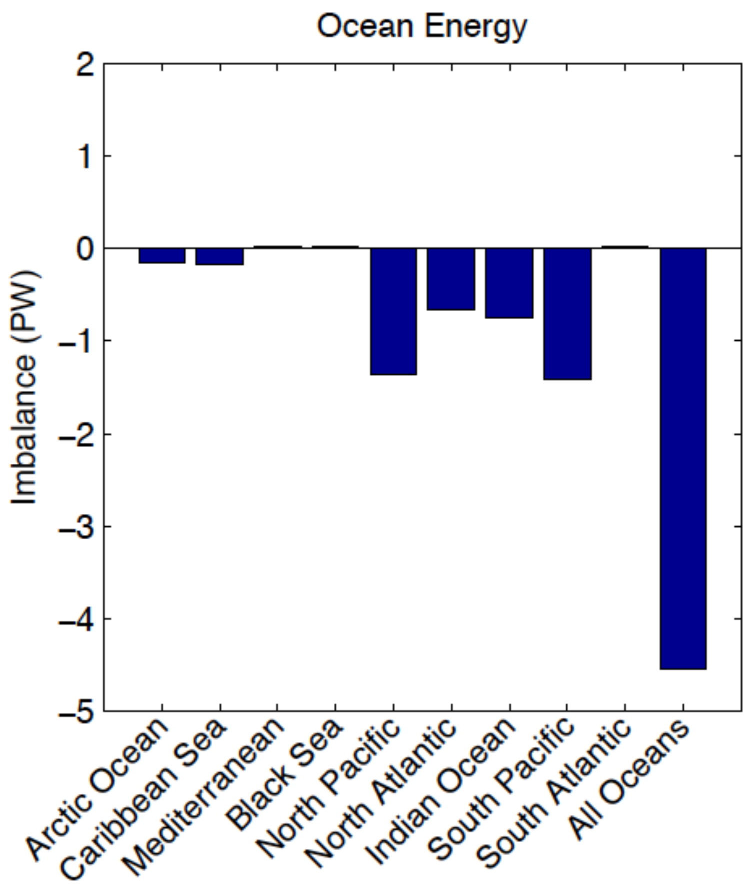

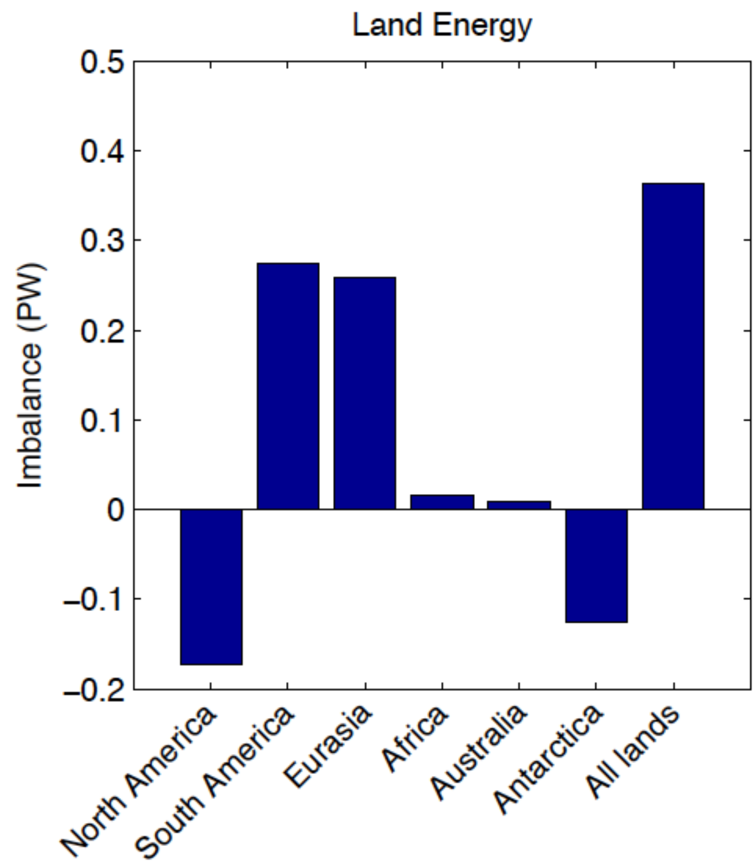

Consistent with L'Ecuyer et al. 2015 who compute surface energy balance

Land sensible heat fluxes are taken from L'Ecuyer et al. 2015 (J. Climate)

Atmospheric energy uncertainty

Estimated annual 1°×1° atmospheric energy uncertainty

Residual divided by the uncertainty

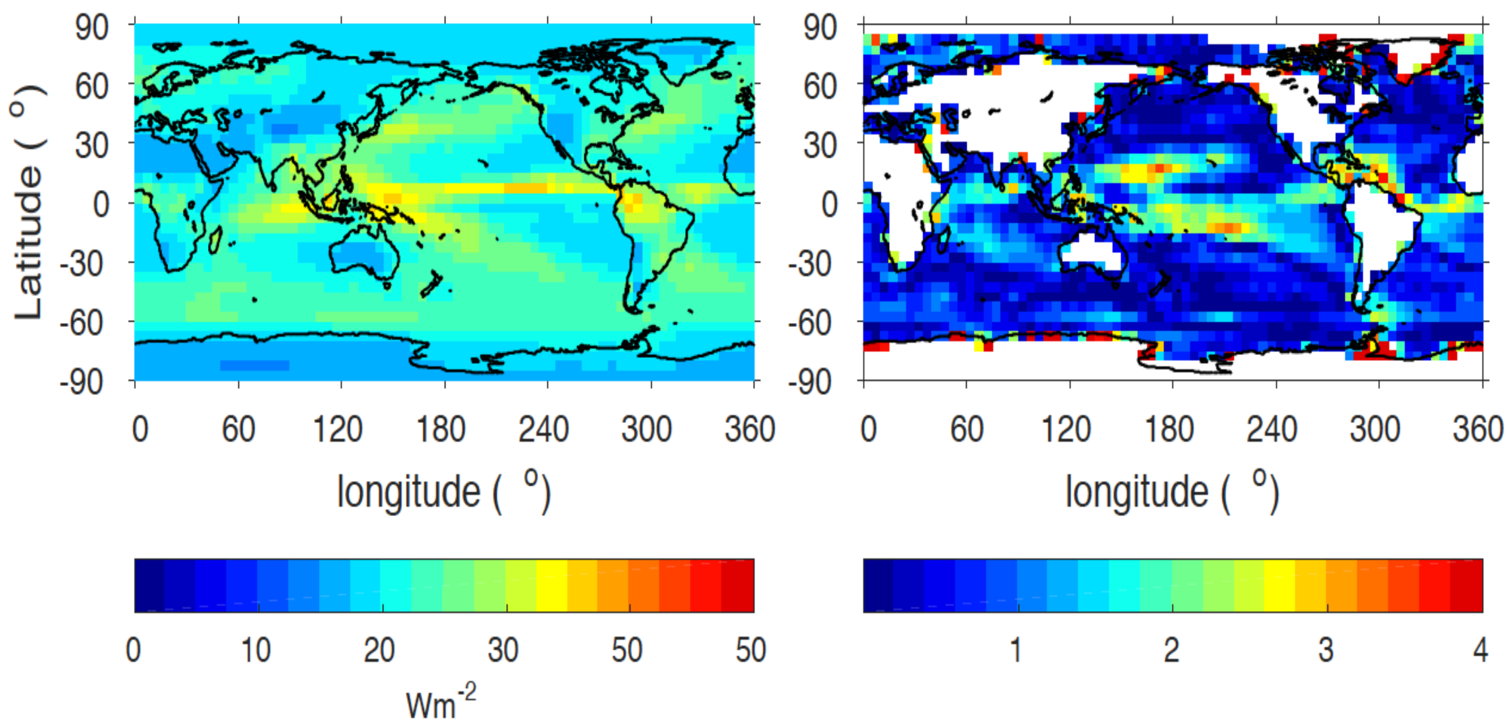

Seasonal atmospheric energy variability

Southern western Pacific (0° to 25°S; 105°E to 180°E)

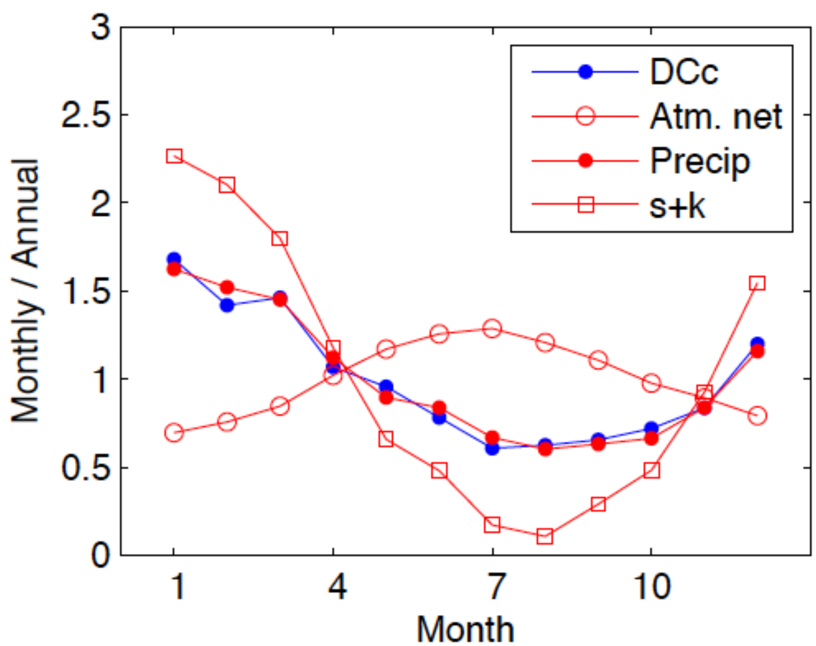

Northern western Pacific (0° to 25°N; 105°E to 180°E)

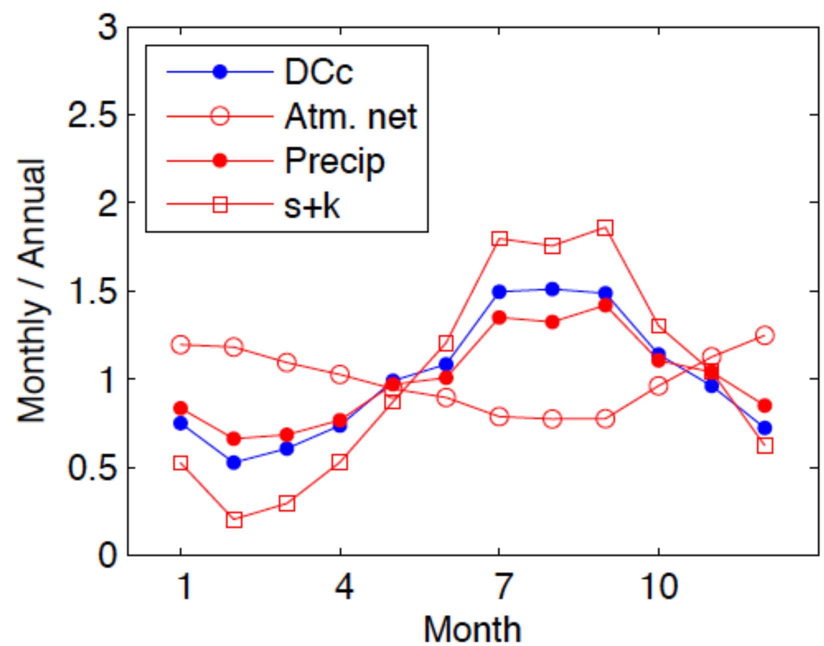

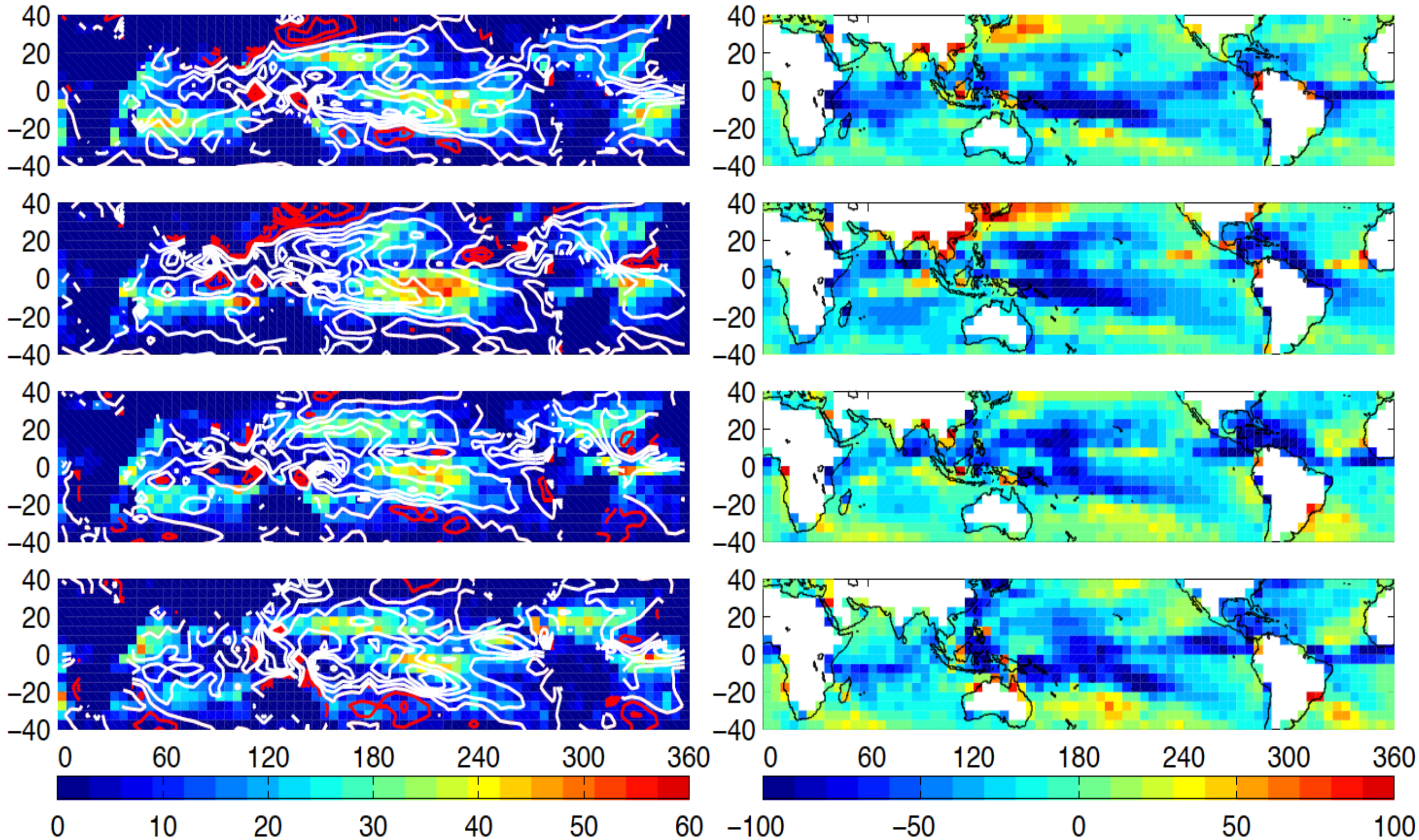
40
20
0
−20
−40
0
60
120
180
240
300
360
0
10
20
30
40
50
60
−100
−50
0
50
100

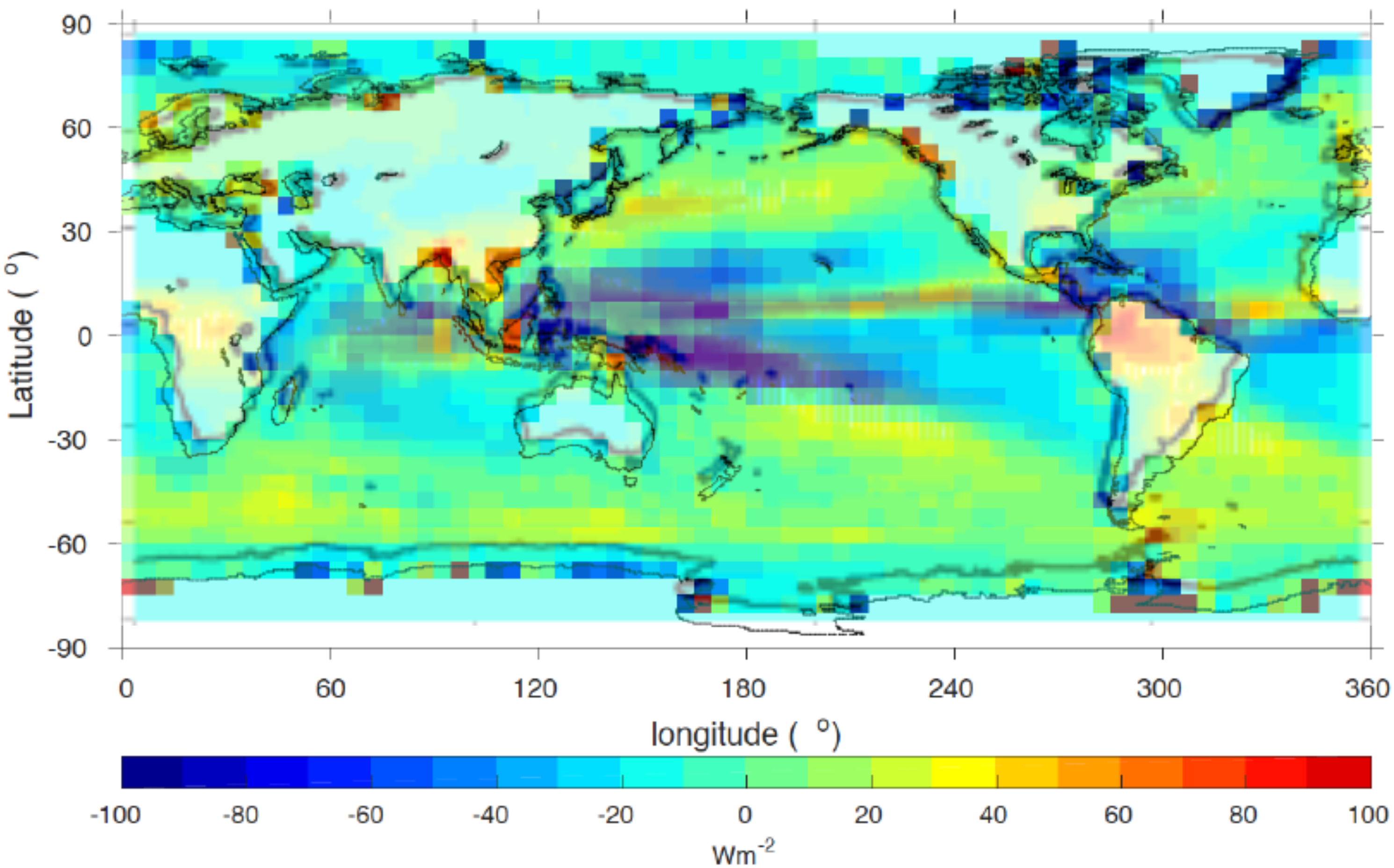

90
60
30
0
-30
-60
-90
Latitude (°)
0
60
120
180
240
300
360
longitude (°)
-100
-80
-60
-40
-20
0
20
40
60
80
100
Wm-2